Available online at www.sciencedirect.com

ScienceDirect

Procedia Engineering 130 (2015) 1327 – 1342

Procedia Engineering

www.elsevier.com/locate/procedia

14th International Conference on Pressure Vessel Technology

# Comparisons of the Solutions of Common FFS Standard Procedures to Benchmark Problems

N.O. Larrosa[a,*], R.A. Ainsworth[b]

[a]School of Materials, The University of Manchester, Manchester M13 9PL, UK
[b]School of Mechanical, Aerospace & Civil Engineering, The University of Manchester, Manchester M13 9PL, UK

**Abstract**

The common practice in industry to assess the severity of crack-like defects in structural components is to follow methodologies usually compiled within standardised procedures or codes. The most popular Fitness-For-Service (FFS) procedures are (1) the UK nuclear industry standard for fracture assessment R6, (2) the American Petroleum Institute FFS procedures, API 579, and (3) the British Standards Institution assessment procedure, BS7910. These codes usually assess structural integrity by means of the Failure Assessment Diagrams (FAD) in which elastic fracture and plastic collapse are assessed independently and combined in a graphical way. Due to the formulations within the codes being different, some divergence is expected in the results provided. The aim of this paper is to show the differences in the results in the assessment of two candidate problems assessed by the API 579, R6 and BS 7910 procedures and to highlight and discuss the possible reasons behind these differences.



Peer-review under responsibility of the organizing committee of ICPVT-14

*Keywords:* Fitness-for-service; FAD solutions; R6; BS 7910; API 579

## 1. Introduction

Different causes may lead to the failure of pressure vessels and piping in service. Fracture, corrosion, creep, fatigue, plastic collapse, and their interaction, are examples of failure mechanisms that are likely to contribute to component degradation and potential failure. Therefore assessing the severity of defects at given loading conditions is essential

* Corresponding author. Tel.: +44-(0)161-306-4286.
*E-mail address:*nicolas.larrosa@manchester.ac.uk



Peer-review under responsibility of the organizing committee of ICPVT-14
doi:10.1016/j.proeng.2015.12.303

in order to evaluate structural integrity. Traditionally, the tolerable size of defects was set by workmanship-based criteria that were somewhat arbitrary and always conservative, sometimes excessively so.

Decades of research and industrial experience together with extensive technical peer review has led to the development and compilation of standardised routes for the evaluation of structural integrity of defective components/structures. In these, acceptance levels for flaws are related to the loading on the structure and to material properties.

Different procedures based upon the principle of fitness-for-service have been created by international organizations and are well accepted in most industries. The most popular procedures are (i) the API 579-1/ASME FFS1 [1], developed by the American Petroleum Institute (API), (ii) BS 7910 [2], which is the general UK procedure for the assessment of flaws in metallic structures developed by the British Standard Institution (BSI) and (iii) the R6 procedure [3] which is the UK nuclear industry flaw assessment technique, originated by the former CEGB, developed by the former British Energy, and now under the direction of EDF Energy.

These procedures usually evaluate fitness-for-service of components containing crack-like defects by means of Engineering Critical Assessments (ECA). ECA is based on damage tolerance principles (fracture mechanics) and is used to assess whether or not a defective component is in a safe condition from elastic-plastic fracture and plastic collapse under specified loading and environmental conditions.

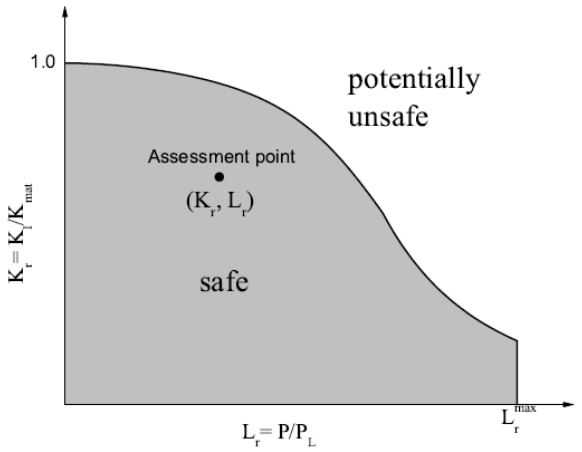


Fig. 1. Failure assessment diagram illustrating safe region bounded by the FAD curve and cut-off.

The failure assessment diagram (FAD) provides a graphical representation of the limiting value of the normalised driving force as a function of the normalised applied load. In general, the shape of the curve depends on the material properties and geometry of the component under analysis. However, simplified FAD curves, independent of geometry and material data, have been derived by applying conservative assumptions, [1–3]. More sophisticated routes, requiring material specific data (e.g., stress-strain curve, tearing resistance curve) can also be used. These different approaches provide different levels of assessment, are of increasing complexity and require experience and more expert engineering judgement.

The aim of the present work is to highlight differences in the results in the assessment of the same problem by means of three different procedures. A FAD-based analysis is used to evaluate fitness for service of 2 different case studies by means of the material and geometry independent failure assessment curve, usually known as the Option 1 Failure Assessment Curve. Qualitative variations in the procedures as well as quantitative differences in results and the level of conservatism are reported for the cases under analysis. Finally the benefits and limitations of applying each of the methodologies are discussed.

**Nomenclature**

| | |
|---|---|
| $2a$ | crack depth |
| $B$ | specimen thickness |
| $2c$ | crack length |
| $E$ | elastic modulus |
| $F^L$ | reserve factor on load. |
| $K_I$ | mode I stress intensity factor |
| $K_I^P$ | stress intensity factor due to primary loads |
| $K_I^S$ | stress intensity factor due to secondary loads |
| $K_{mat}$ | fracture toughness |
| $K_r$ | fracture ratio |
| $K_r^P$ | fracture ratio due to primary loads |
| $K_r^S$ | fracture ratio due to secondary loads |
| $L_r$ | non-dimensional plastic collapse parameter |
| $L_r^{\max}$ | non-dimensional plastic collapse parameter cut-off value |
| $P$ | internal pressure |
| $P_L$ | collapse pressure |
| $Q_m$ | secondary membrane stress |
| $Q_b$ | secondary bending stress |
| $r_i$ | internal radius |
| $r_m$ | mean radius |
| $r_o$ | outer radius |
| T | operating temperature |
| V | plasticity interaction factor |
| $\sigma$ | stresses due to applied loads |
| $\sigma_{ref}$ | reference stress |
| $\sigma_f$ | flow stress |
| $\sigma_{ys}$ | yield stress |
| $\sigma^r$ | residual stress profile |

## 2. FAD-based comparison

The objective of this work is to highlight differences in FFS assessment procedures in assessing the significance of crack-like defects by focusing on stress intensity factor (SIF) and plastic collapse solutions as well as the significance in the assessment of considering residual stresses and how the procedures account for the effects of residual stresses on the crack driving force. The FAD, Fig. 1, is the most widely used approach for assessing the integrity of structures containing crack-like defects, so comparisons will be made based on the FAD-framework where assessment results are plotted in the FAD providing a simple and straightforward way of showing the driving force for both plastic collapse and elastic-plastic fracture mechanisms and to compare solutions among the codes. For comparison purpose, the effects of other features (e.g. partial safety factors, material property estimation, etc.) that may also affect results are excluded in the analyses.

The solutions used in this work were the best available in each procedure for the SIF and plastic collapse solutions. That is, if say a SIF solutions was not available for a cylinder under analysis but a plastic collapse solution was, then a flat plate solution was used for the SIF calculation with a cylinder solution for plastic collapse to obtain the assessment point ($K_r$, $L_r$).

## 3. Benchmark problems

In this work 'Example Problem 9.5' and 'Example Problem 9.6' from [4] have been considered. These address the assessment of an internal surface flaw in the axial weld of a pipe/cylinder and a fully circumferential crack-like flaw in the girth weld on the outside surface of a pipe/cylinder, respectively. These examples are labelled hereafter 'Case study 1' and 'Case study 2', Fig. 2.

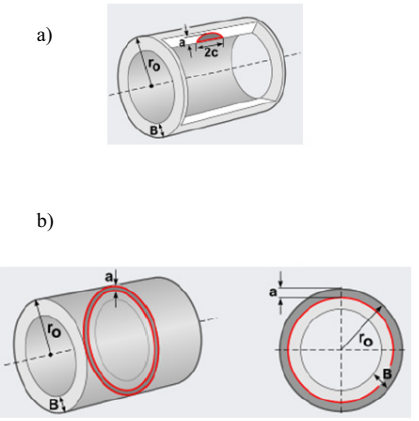


Fig. 2. Geometries considered for the comparison of the FFS assessment procedures: (a) 'Case study 1'; (b) 'Case study 2'. Figures obtained from *Crackwise*® [5] library.

### *3.1. Case study 1*

The first example is that of a crack-like defect located in the heat affected zone (HAZ) parallel to a longitudinal double V-groove seam, on the inside surface of a cylindrical pressure vessel. The pressure vessel is made of SA-516 Grade 70 steel and designed as per the ASME B&PV code, Section VIII, Division 1, 1998. The cylinder is fully pressurised when temperature T≥40$^o$F to an internal pressure $P$=200 *psig*. The vessel is not subject to post weld heat treatment (PWHT) at the time of fabrication. [Note, the benchmark problems in [4] are provided in Imperial units but assessments are generally reported here in non-dimensional form or converted to SI units where necessary.]

The detected flaw depth $a$=5.08 mm is estimated from ultrasonic testing (UT) and its length 2$c$=81.28 mm is obtained by means of the magnetic particle inspection technique (MT) as reported in [4]. The outside radius and the thickness of the cylinder are $r_o$=61 *in* and $B$=1 *in*, respectively, so that the internal radius is $r_i$=60 *in*. Table 1 shows the material properties used in the assessment. For a more detailed description of the problem the reader is referred to [4].

Table 1. Material properties of the steel in "Case Study 1".

| Property | Magnitude |
|---|---|
| Young's modulus E (GPa) | 206 |
| Poisson's ratio | 0.3 |
| Minimum specified yield stress $\sigma_{ys}$ (ksi) | 5 |
| Fracture toughness Kmat (ksi in0.5) | 85.9 |

Thin-walled cylinder solutions ($B/r_o$=0.0167) are used to compute the hoop ($\sigma_m$) and through-wall bending ($\sigma_b$) components of the primary stress at the centre of the uncracked cylinder, using equations (D.47) and (D.48) in [1]:

$$\sigma_m = \frac{P.r_i}{B} = 12\ ksi = 82.74\ \text{MPa} \tag{1}$$

$$\sigma_b = \frac{P.r_o^2}{r_o^2 - r_i^2}\left[\frac{B}{r_i} - 1.5\left(\frac{B}{r_i}\right)^2 + 1.8\left(\frac{B}{r_i}\right)^3\right] = 0.1\ ksi = 0.6894\ \text{MPa} \tag{2}$$

Due to its small value in comparison to the membrane stress component $\sigma_m$, the bending stress $\sigma_b$ is neglected in the assessment. A Partial Safety Factor on load of 1.5 is used in the solution provided in [4]. Thus in the assessments reported here $\sigma_m$=82.74 MPa * 1.5= 124.1 MPa is used, to make results directly comparable to the benchmark results in [4].

Residual stresses are accounted for means of a uniform membrane surface residual stress distribution. The simple and conservative approaches are given in equations (3)-(5):

$$\sigma^r(y) = \sigma^r_{ys} R_r \ \text{ with } \sigma^r_{ys} = \sigma_{ys} + \Delta\sigma_{ys} \quad \text{(API 579)} \tag{3}$$

$$\sigma^r(y) = \min\left[\sigma_{ys}, \left(1.4 - \frac{\sigma_{ref}}{\sigma_f}\right)\sigma_{ys}\right] \quad \text{(BS 7910)} \tag{4}$$

$$\sigma^r(y) = \sigma_{ys} \quad \text{(R6)} \tag{5}$$

where $y$ is the local coordinate for the stress distribution along the outer surface and is measured from the weld centre and perpendicular to the seam direction. In equation (3), $R_r$ is a reduction factor accounting the effect on residual stresses of the test pressure. According to the API 579 procedure (Eqs. E.33-35 in [1]), for this case $R_r$ =1. The elevation of the membrane residual stress in API 579, $\Delta\sigma_{ys}$ = 10 *ksi* =69 MPa, is given in Eq. E.1-2 in [1] with $\sigma_{ys}$ in this code being the minimum specified yield stress. In equation (4), $\sigma_{ref}$ and $\sigma_f$ are the reference stress and the flow stress, respectively. In BS7910 and R6, $\sigma_{ys}$ in equations (4, 5) should be taken as the mean yield stress, in contrast to the minimum specified yield stress. However, as [4] does not provide mean yield stress data, the minimum specified yield stress has been used instead when applying BS7910 and R6 and this is discussed later.

Figure 3 shows the range of application of the SIF solutions given in each procedure for a cylinder with a semi-elliptical internal crack. It is worth noting that the ranges of application for the SIF solutions differ significantly among the procedures. For this case, R6 includes solutions for only a limited range of $r_m/B$ but provides a source reference for higher $r_m/B$, the solutions from which are contained in the R-code software. As for the case under analysis (green dot), the SIF solutions contained in both R6 and BS 7910 are outside the range of application, a flat plate solution has been used in the assessment as an alternative. R-code 5.1 software has also been used as it provides the solutions referred to in R6, with a larger range of application. There are no evident dimensional restrictions for the reference stress solutions for this geometry in the procedures. BS7910 contains both thin-walled (P9.2) and thick-walled (P9.6) solutions. However, as the latter is a local solution with crack-face pressure, the thin-walled solution seems to be the appropriate choice. Care should be taken however in the use of the solutions provided by BS 7910 to assess thick-walled cylinders as it has been derived for thin-walled structures [6]. Table 2 shows the solutions used in the comparison of the present case study. For further detail on the solutions the reader may referred to the procedures.

Figure 4 shows the $L_r$ results for different solutions as a function of the normalized crack depth ($a/B$). Cylinder solutions are shown in the figure for both BS 7910 and API 579. Two sets of surface breaking flat plate solutions are also included for BS 7910. In BS 7910, tensile forces can be applied via pin jointed or fixed grip conditions. $L_r$ estimates for the geometry under analysis are shown in Table 3. Results from API 579 (cylinder) and R6 (cylinder, global) are identical. In contrast, BS 7910 (cylinder) estimates are up to 18 % higher than those for API 579 and R6. For larger cracks, the difference among these solutions does not change significantly. The BS 7910 [Flat plate, Fixed

Grip (FG) and Pin Loaded (PL)] solutions are the most pessimistic, with differences within 80% (FG) and 35% (PL). As shown in Fig. 4, differences are larger for higher *a/B* values.

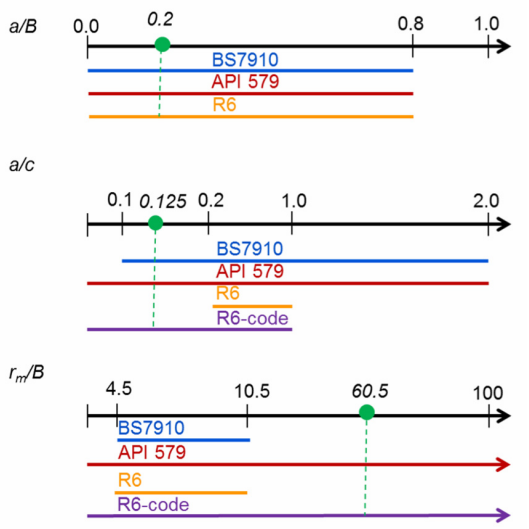


Fig. 3. Stress intensity factor ranges of application for a cylinder with an internal semi-elliptical axial flaw. Green dot represents case under analysis.

Table 2. Solutions used in the assessment for 'Case study 1'. LL: Limit load; RS: Reference Stress; PS: Primary stresses; SS: Secondary stresses; G: Global; L: Local; TW: Thick-walled.

| Procedure | Geometry | SIF | Reference Stress Limit load |
|---|---|---|---|
| R6 | Plate | IV.3.3.1 | |
| | Cylinder | | IV.1.9.1 |
| BS 7910 | Plate | M.4.1 | P.6.1 (RS) |
| | Cylinder | M.7.2.4 | P.9.2 |
| API 579 | Cylinder | C.187(PS) | D.74 (RS) |
| | | C.192(SS) | |

Table 3. Plastic collapse parameter (Lr) results for "Case Study 1". FP: Flat Plate ; FG: Fixed grip ; PL: Pin loaded; Cyl: Cylinder solution ; G: Global ; L: :Local.

| Solution | Lr | Percentage difference (API 579) |
|---|---|---|
| BS 7910(FP-FG) | 0.628 | 29,31% |
| BS 7910 (FP-PL) | 0.866 | 78,25% |
| BS 7910 (Cyl) | 0.573 | 17,92% |
| API 579 (Cyl) | 0.486 | n/a |
| R6 (Cyl) | 0.486 | 0.0% |

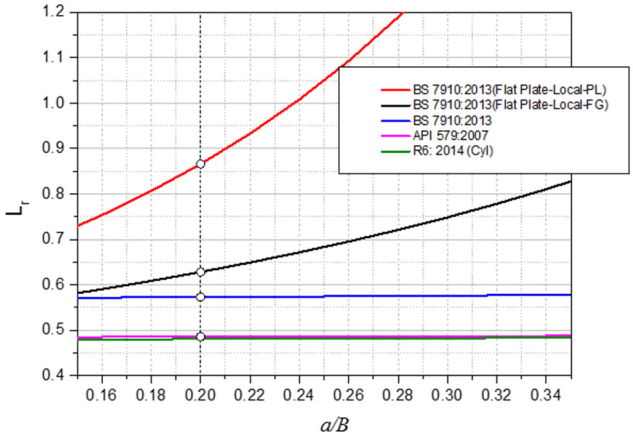


Fig. 4. Plastic collapse ratio ($L_r$) for the solutions provided in the three standards. Vertical dashed line shows results for 'Case Study 1.'

Fracture parameter ($K_r$) estimates for primary and secondary loads and the plasticity interaction factor (V) are shown in Table 4. It is observed that the primary load components ($K_r^P$) are in very close agreement. Significant differences between API 579 secondary loads ($K_r^S$) estimates and R6/BS 7910 predictions are found but this is largely because the residual stress used in API 579 is higher than that used for the BS7910/R6 calculations as a results of the addition of $\Delta\sigma_{ys}$ in equation (3). As shown in the Table, for the case of R6/BS 7910 the ratio of the fracture parameter for secondary loads to that of primary loads ($K_r^S/K_r^P$) is almost the same as the ratio of the membrane residual stresses to the applied membrane stress ($\sigma_y^r/\sigma$), showing that for this simplified case, the same SIF solution is used for the pressure membrane stress and the residual stress. A difference of 2.5% between $K_r^S/K_r^P$ and $\sigma_y^r/\sigma$ is observed in API 579, indicating that the SIF solutions used for the primary and secondary loads differ, although not significantly.

Table 4. Fracture parameter results for primary (KrP ) and secondary (KrS ) loads for "Case Study 1".

| | R6 | BS 7910 | API 579 |
|---|---|---|---|
| $K_r^P$ | 0.195 | 0.197 | 0.198 |
| $K_r^S$ | 0.413 | 0.416 | 0.516 |
| $K_r^S/K_r^P$ | 2.118 | 2.112 | 2.601 |
| $\sigma_y^r/\sigma$ | 2.111 | 2.111 | 2.667 |
| V | 1.118 | 1.167 | 1.145 |

Table 5 shows the results of the assessment for the surface ($\phi$=0º) and deepest points ($\phi$=90º) of the axially oriented internal crack, both including and excluding the effect of residual stresses. Using the API 579 solution as an arbitrary reference, when a uniform residual stresses distribution is taken into account, $K_r$ solutions are within 18% for the deepest point and within 4% for the surface point. If residual stresses are neglected, solutions are within 2% and 15% at the deepest and the surface point, respectively. Differences in $L_r$ solutions are within 18%. The largest differences arises between BS7910, a limit load approach, and the solutions provided by R6 and API579 which are based on a references stress approach, and are expressed by similar equations. Fig. 5 shows these results within the Option 1 failure assessment diagram (FAD).

Table 5. Plastic collapse parameter (Lr) and fracture parameter results (Kr) for "Case Study 1".

| Residual stresses | | | Percentage difference (API 579) | |
|---|---|---|---|---|
| *Deepest point* | $L_r$ | $K_r$ | $L_r$ | $K_r$ |
| API 579 | 0.486 | 0.799 | n/a | n/a |
| R6 | 0.486 | 0.657 | 0.0 % | -17.84% |
| BS 7910 | 0.573 | 0.682 | 17.91% | -14.71% |
| *Surface point* | Lr | Kr | $L_r$ | $K_r$ |
| API 579 | 0.486 | 0.274 | n/a | n/a |
| *R6* | 0.475 | 0.265 | 0.0 % | -3.36% |
| BS 7910 | 0.573 | 0.268 | 17.91% | -2.10% |
| No residual stresses | | | Percentage difference (API 579) | |
| *Deepest point* | Lr | Kr | $L_r$ | $K_r$ |
| API 579 | 0.486 | 0.198 | n/a | n/a |
| *R6* | 0.475 | 0.195 | 0.0 % | -1.49% |
| BS 7910 | 0.573 | 0.197 | 17.91% | -0.77% |
| *Surface point* | Lr | Kr | $L_r$ | $K_r$ |
| API 579 | 0.486 | 0.069 | n/a | n/a |
| R6 | 0.475 | 0.079 | -2.24% | 14.41% |
| BS 7910 | 0.573 | 0.078 | 17.91% | 12.47% |

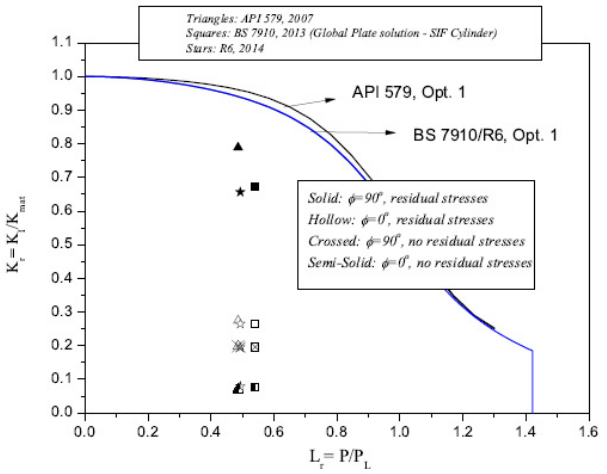


Fig. 5. Assessment results of 'Case study 1'at the surface ($\phi$=0$^O$) and deepest point ($\phi$=90$^O$) locations with and without the effect of residual stresses.

It was noted above and shown in Eq. (3) that API 579 [1] recommends an elevation above the minimum specified yield strength to account for the typical elevation of material properties above minimum requirements. In Fig. 6, the red symbols show the API 579 solutions if this elevation is not considered. It is observed that the points are shifted downwards and the $K_r$ solutions at the deepest point, where conditions are most severe, differ by less than 2.5% from the other solutions. Using the same value of the membrane residual stress as that in R6/BS7910 procedures, API 579 estimates $K_r^S/K_r^P$ =2.056 , with $\sigma_y^r/\sigma$ = 2.111 (see Table 4).

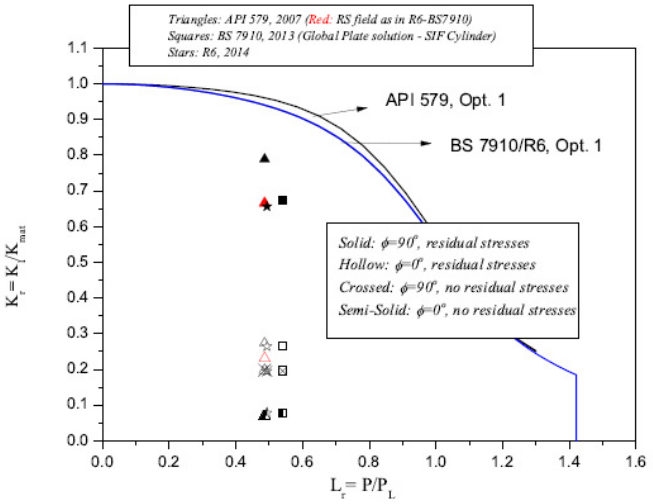


Fig. 6. Assessment results of 'Case study 1'at the surface (ϕ=0o) and deepest point (ϕ=90o) locations with and without the effect of residual stresses. Red symbols shows assessment using membrane residual stresses as recommended in R6/BS 7910.

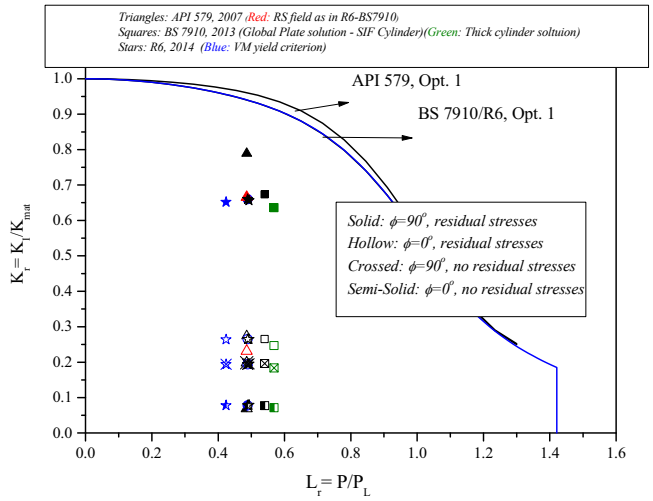


Fig. 7. Assessment results of 'Case study 1'at the surface ($\phi$=0$^O$) and deepest point ($\phi$=90$^O$) locations with and without the effect of residual stresses. Conditions 1 and 2 plotted.

Figure 7 shows results for two additional conditions: 1) adjusting the pipe dimensions and value of the applied internal pressure ($P$) to keep the same applied membrane stress and obtain a ratio $r_m/B$ that fits within the thick pipe SIF solutions range (Fig. 2); 2) adopting the Von Mises yield criterion.

The extreme values, $r_m/B$=10.5 and $r_m/B$=4.5, were used in the comparison to assess the effect on the results and the value of $P$ was obtained accordingly from Eq. (1). The results for these 2 cases differ by less than 0.02% in $L_r$ and 0.69 % and 1.62% in $K_r$ at the base and the edge of the crack, respectively. As a result, estimates for $r_m/B$=10.5 are only plotted in the figure. In comparison with the flat plate solutions, results for condition 1 are higher in terms of

plastic collapse parameter ($L_r$) ,within 5.25%, and lower in terms of the fracture parameter ($K_r$), with differences of less than 9% for the edge of the crack and within 6.5% at the base of the flaw.

For condition 2, $L_r$ results using the von Mises yield criterion (blue stars) are lower than those obtained by the Tresca yield criterion (black stars) but differ by less than 14%.

Figure 8 shows the reserve factors ($F^L$) for the surface and the deepest point of the crack when residual stresses are taken into account and when they are neglected. It is observed that the value of $F^L$ is considerably higher when the effects of residual stresses are not considered in the analysis and it is significantly lower when they are included, with a value very close to 1 in the case of API 579 at the base of the flaw.

Finally, Fig. 9 shows the critical crack sizes estimated with the different codes. Generally, BS 7910 provides the most pessimistic results, whereas R6 and API 579 show higher and very similar estimates.

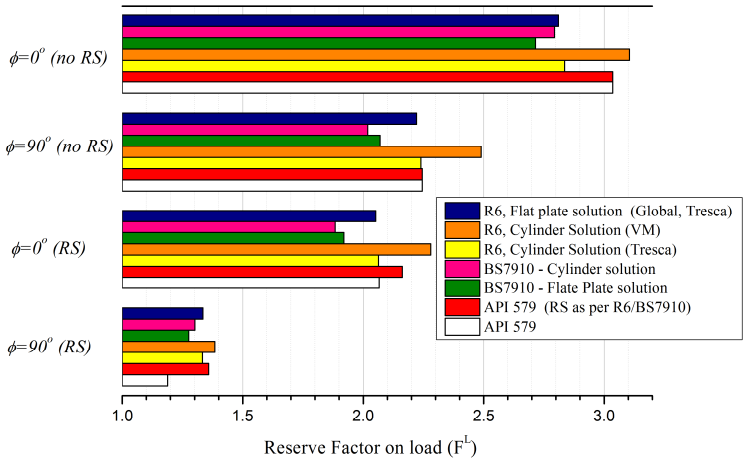


Fig. 8. Reserve Factors on Load for 'Case study 1'. Comparison of assessment procedure estimations.

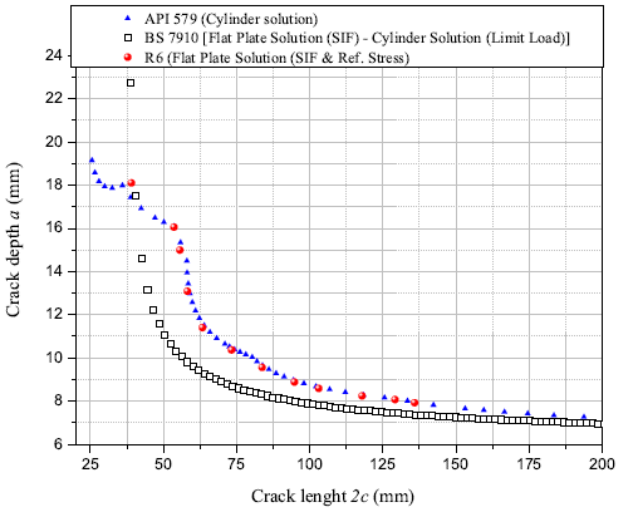


Fig. 9. Critical crack size estimations for 'Case study 1'. Comparison of assessment procedure estimates.

### 3.2. Case study 2

Case study 2 is a crack-like flaw that has been found on the outside surface of a pipe at the weld toe of the girth weld pipe, Fig. 2(b).The seam is a single V-groove weld and the flaw is parallel to the weld seam. The pipe is made of SA-516 Grade B steel and designed as per ASME B31.3 code, 2003. Fully operational conditions are reached when T=20ºC. The pipe was designed to sustain 3 MPa of internal pressure at 250ºC and had not been subject to post weld heat treatment (PWHT) at the time of fabrication (no relaxation of residual stresses). The detected flaw depth is a=3 mm. The outside radius and the thickness of the cylinder are $r_o$=254 mm. and $B$=9.53 mm, respectively.

Internal pressure and global bending due to the location of the flaw (midway between 2 supports which are at a distance apart of 10.5 m) are taken into account. The selected heat input corresponds to shielded metal arc welding (SMAW)/metal arc welding (MMA) passes recorded as $E_1$ = 1500 Joules/mm. Table 6 shows the material properties used in the assessment.

Table 6. Material properties of the steel in "Case Study 2".

| Property | Magnitude |
|---|---|
| Young's Modulus $E$ (GPa) | 206 |
| Poison's ratio $v$ | 0.3 |
| Minimum specified yield stress $\sigma_{ys}$ (MPa) | 240 |
| Fracture toughness $K_{mat}$ (MPa.m$^{0.5}$) | 111.47 |

Figure 10 shows the range of application for the SIF solutions for 'Case study 2', a cylinder with a fully circumferential external crack for each procedure. For the case under analysis (green dot), the SIF solutions provided by R6 is out the range of application, thus a flat plate solution was used for assessment purpose. However, as for Case study 1, R6 provides a source reference for solutions for larger $r_m/B$ and these solutions are contained in R-code.

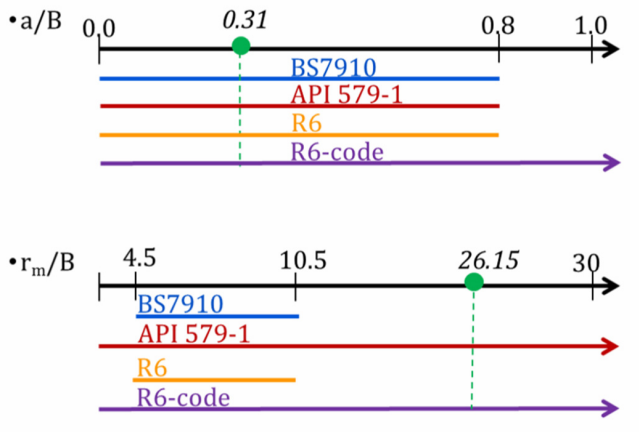


Fig. 10. Stress intensity factor ranges of application for a cylinder with an external circumferential flaw. Green dot represents case under analysis.

Table 7 shows the SIF and reference stress/limit load solutions used in this case study. In this problem the treatment of secondary stresses (i.e., residual stresses) is done by using a non-uniform stress distribution across the thickness of the pipe, in contrast to 'Case study 1', where a constant residual stress distribution was used.

Table 7. Solutions used in the assessment for 'Case study 2'. LL: Limit load; RS: Reference Stress.

| Procedure | Geometry | SIF | Reference Stress or Limit load |
|---|---|---|---|
| R6 | Plate | IV.3.3.1 or IV.3.3.2 | |
| | Cylinder | | IV.1.8.1 (LL) |
| BS 7910 | Cylinder | M.7.3.5 | P.10.5 (RS) |
| API 579 | Cylinder | C.178 | D.63 (RS) |

Here, comparisons of the results by using the different procedures and the recommended residual stress profiles given illustrates the impact of the assumed residual stress profiles on the assessment results as well as the effect of the SIF solution on the assessment results for the same non-uniform residual stress profile.

The transverse residual stress profile (perpendicular to the weld) in BS 7910 Annex Q and R6 Section IV.4 suggest three types of profile depending on the material (ferritic or austenitic) and welding heat input energy. For the case of API 579, the through-thickness residual stress field is calculated from Annex E.4 as a function of the mean radius to thickness ratio and of the heat input of the welding process and it is provided as the superposition of a 'linear' and a self-equilibrating component. Both BS 7910 and R6 only consider wall thickness effects in a normalized linear heat input definition, while API 579 RP-1/ASME FFS-1 explicitly incorporate thickness term in the residual stress formulation up to a thickness of 50 mm. The transverse residual stresses suggested for the different procedures are shown in Fig. 11.

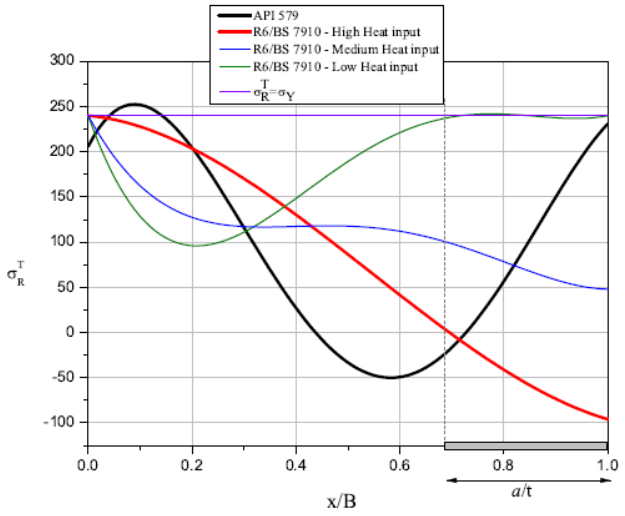


Fig. 11. Transverse residual stress profiles prescribed by API 579 (Annex E), BS 7910 (Appendix Q) and R6 (Sec. IV.4).

A simple and rapid approach to assess stress intensity factor solutions, for both primary and secondary loads, is to take into account stress gradients by linearising the stress field over the flaw depth, $a$, and splitting it into membrane (tensile) and bending components. The method of linearisation should be pessimistic in that SIFs are overestimated [2,3].

Figure 12 shows the stress linearisation approach used as suggested in R6 and BS 7910. It is observed that there are compressive residual stresses over the complete crack face, giving a positive membrane stress ($Q_m$) and a negative bending component ($Q_b$).

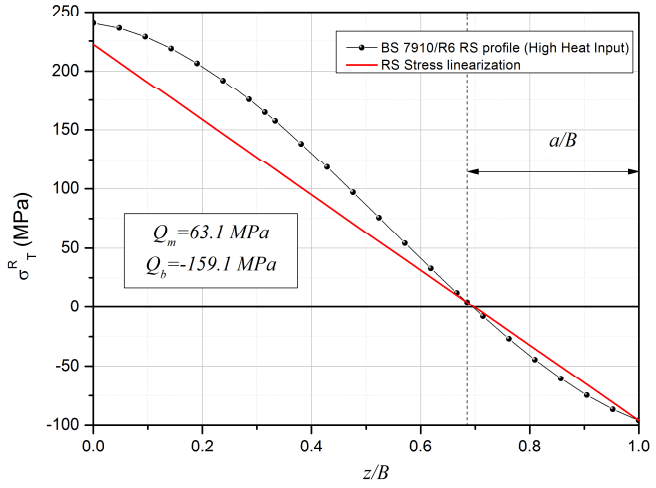


Fig. 12. Stress linearisation approach used to assess residual stress crack driving force.

Figures 13 and 14 shows the fitting approach used to evaluate the SIF for the case under analysis. Third-order (Fig. 13) and a fourth-order (Fig. 14) polynomial fits are used to obtain SIFs with R6 [3] and API 579 [2], respectively. In order to compare solutions of the different approaches suggested in the codes, the linearisation approach is used to obtain SIFs with BS 7910 [1].

Assessment results are shown in Table 8 and Fig. 15. As shown, residual stresses have a significant effect on fracture parameter results. Uniform residual stresses produce the most pessimistic results, whereas the non-uniform distributions usually have a milder effect. It is worth mentioning that application of both R6 and BS 7910 leads to compressive secondary stress intensity factors and for assessment purposes the contribution to the fracture driving force is then neglected ( $K_r^S = 0$ ).

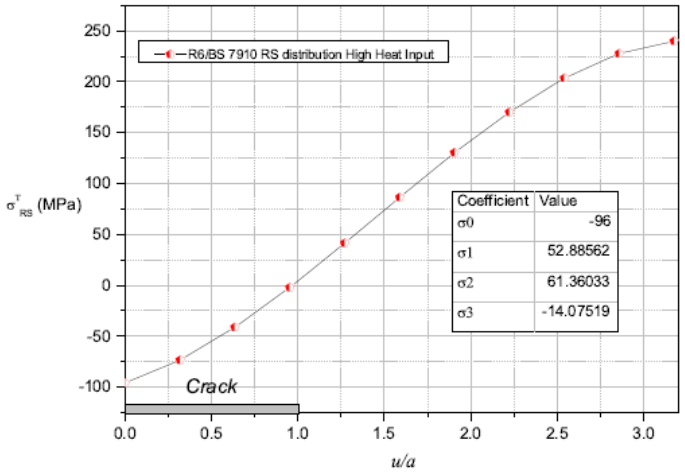


Fig. 13. Third-order polynomial fit to assess residual stress crack driving force, as suggested in R6 (IV.3.1.1) and in BS 7910 (Q.7).

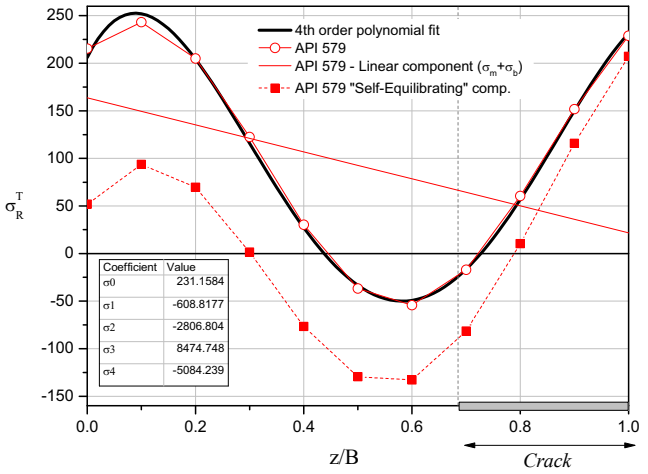


Fig. 14. Fourth-order polynomial fit to assess residual stress crack driving force, as suggested in API 579 (E.4.1.1.b).

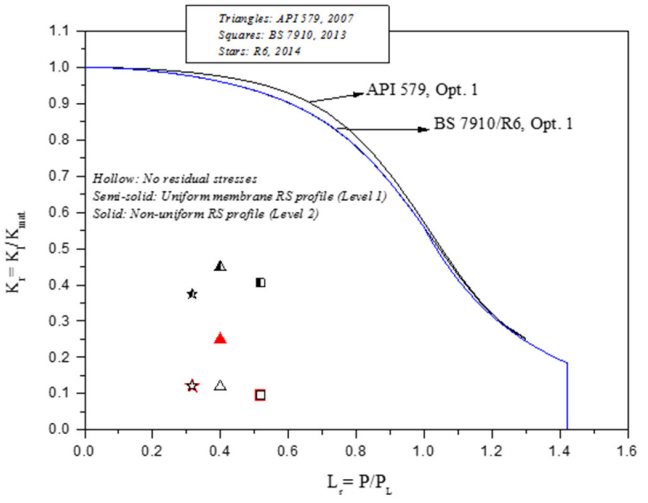


Fig. 15. Assessment results of 'Case study 2' at the deepest point location with and without the effect residual stresses. Comparisons of using a uniform and a non-uniform residual stress profile are shown.

From Table 8 it is observed that $L_r$ solutions are within 30% of each other. R6 $K_r$ solutions were up to 52% and 2% and BS 7910 $K_r$ solutions were up to 62% and 20%, with and without RS respectively, in comparison with API 579 solutions. The difference in SIF due to primary stresses is within 20 %, but much greater differences occur with RS because of both differences in RS levels in the codes and differences in the SIF solution approaches.

Table 8. Assessment results for 'Case study 2'. Effect of 'Level 1' and 'Level 2' residual stress effect in $K_r$ included. Percentage difference with respect to API 579 estimations in parenthesis.

| | Lr | Kr |
|---|---|---|
| | No Residual Stresses | |
| API 579 | 0.3991 | 0.1189 |
| R6 | 0.3163 (-20.75) | 0.1213(1.97) |
| BS 7910 | 0.5170 (29.54) | 0.0963 (-19.06) |
| | Uniform Residual Stress profile (Level 1) | |
| API 579 | 0.3991 | 0.4483 |
| R6 | 0.3163 (-20.75) | 0.3756(-16.23) |
| BS 7910 | 0.5170 (29.54) | 0.4052 (-9.61) |
| | Non-uniform Residual Stress profile (Level 2) | |
| API 579 | 0.3991 | 0.2496 |
| R6 | 0.3163 (-20.75) | 0.1213(-51.40) |
| BS 7910 | 0.5170 (29.54) | 0.0963 (-61.42) |

## 4. Discussion

The assessment results for the two case studies in this work show a number of features. In terms of the availability of geometry specific solutions, API 579 covers a wide range of dimensions for the cases under analysis in this work. As an alternative, flat plate solutions have been used in the application of R6 and BS 7910 due to the dimensions of the cylinders being out of the geometry range covered by the geometry-specific solutions contained in those codes.

It is shown in this paper that neglecting residual stress has a major impact on the assessment solutions and that the approach used to account for residual stresses also plays a major role. For example, API 579 suggests an elevation of the effective yield strength above the specified minimum yield strength to account for the typical elevation of actual properties above minimum requirements. On the other hand, R6/BS 7910 recommend the use of mean values of yield stress. However, if only the value of the minimum specified yield strength, a design material parameter, is available then an estimate of mean yield stress may not be possible. The different recommendations in the procedures on the treatment of residual stresses to evaluate $K_r^s$ have been shown to produce significant differences in $K_r$ estimates. However, using the same approach to account for residual stresses, reduces these differences considerably.

The main differences in $K_r$ solutions arise from differences in SIF formulation solutions and the treatment of secondary stresses. The non-uniform residual stress profile suggested in API 579 is considerably different to that recommended in R6/BS7910. When the crack lies on the external side of the pipe/cylinder, as in 'Case Study 2', a compressive residual stress component is given by R6/BS7910, whereas a tensile residual stress profile is obtained by means of the distribution suggested by API 579. This has a huge impact on the assessment results. For example, although the approach used with R6 and API 579 to assess SIFs is similar, it is observed that the severity of the defect is unchanged (as $K_r^S < 0$ it is set to zero) when applying the non-uniform residual stress profile as suggested in R6/BS 7910 (compressive stresses on the area where the crack lies), whereas an increased severity is obtained when applying the API 579 residual stress profile (tensile stresses on the area where the crack lies).

Significant differences in $L_r$ solutions arise due to the availability of geometry-specific solutions. Adjusting the pipe dimensions and value of the applied internal pressure ($P$) to keep the same applied membrane stress and obtain a ratio $r_m/B$ that fits within the thick pipe SIF solution range (Fig. 2) led to results in good agreement with each other.

## 5. Conclusions

In this work, results based on 3 of the most commonly used Fitness-For-Service procedures have been compared to assess the significance of defects by focusing on SIF and plastic collapse solutions, The same loading conditions

and material properties have been used in application of all codes to exclude some of the effects of other features (e.g. partial safety factors, material properties estimation, etc.) that may affect results.

Example problems 9.5 and 9.6 from API 579-FFS2 [4] were used as benchmarks. Example problem 9.5 consists of a crack-like flaw parallel to a longitudinal double V-groove seam weld on the inside surface of a cylindrical pressure vessel under internal pressure, whereas Example problem 9.6 evaluates a crack-like flaw in a circumferential seam on the outside surface of a pipe under internal pressure and global bending.

In these analyses, it was observed that:

- The API 579 standard contained solutions for the largest range of dimensions for the cases under analysis.
- $L_r$ results derived by BS 7910 are higher than the other codes.
- Differences in SIF formulation solutions, V factor and residual stresses lead to significant variations in $K_r$ solutions.
- In R6/BS 7910, a Level 1 treatment of residual stresses assumes that the magnitude of welding residual stress is the mean yield strength of the parent material. API 579 provides an elevation of the effective yield strength above the specified minimum yield strength to account for the typical elevation of actual properties above minimum requirements.
- For Case study 2, the Level 2 non-uniform residual stress distribution suggested by API 579,for the specific level of heat input given, is significantly different from those in R6 and BS7910.
- Both, a stress linearisation approach and a polynomial fitting procedure are suggested in R6 and BS 7910 to assess stress intensity factors in flat plates.
- BS 7910 SIF solutions were assessed in this work in terms of bending and membrane stress. R6 and API 579 solutions are presented in terms of weight functions, allowing stress intensity factors to be evaluated for arbitrary stress fields.
- The stress linearisation approach is quick and easy, and provides a satisfactory preliminary solution.
- The polynomial curve fitting approach, used in 'Case Study 2' to assess the $K_r$ solution by means of R6 and API 579 usually requires fitting the stress field by $4^{th}/5^{th}$ order polynomials. For some geometries, numerical integration for the calculation of the *SIF* is also needed.

This paper is part of an on-going project and these are preliminary results.

## Acknowledgements

The authors wish to acknowledge part-funding for this research from B.P. through the B.P. International Centre for Advanced Materials. Provision of software by TWI, EDF Energy and Quest Integrity is gratefully acknowledged.

## References

[1] American Petroleum Institute/ American Society of Mechanical Engineers, API 579/ASME FFS-1, Recommended practice for fitness-for-service, API, 2007.
[2] BS 7910:2013. Guide to methods for assessing the acceptability of flaws in metallic structures. British Standard Institution, London, UK, 2013.
[3] R6, Revision 4, Assessment of the integrity of structures containing defects. EDF Energy, Gloucester, UK, 2015.
[4] API 579-2/ASME FFS-2 2009 Fitness-for-service Example problem manual, API, 2009.
[5] Crackwise 5.1 - Automation of Fracture and Fatigue Assessment Procedures (BS 7910) for Engineering Critical Assessment, 2014
[6] Eren, S., Hadley, I., and Nikbin, K., 2011. Differences in the assessment of plastic collapse in BS 7910:2005 and R6/Fitnet FFS procedures. American Society of Mechanical Engineers, Pressure Vessels and Piping Division PVP, Vol. 1, pp. 791–818.